Molecular Crystals and Liquid Crystals
Publication details, including instructions for authors and subscription information:
http://www.tandfonline.com/loi/gmcl16

Molecular Alignment of Bubble Domains in Large Pitch Cholesteric Liquid Crystals

Tadashi Akahane [a] & Toshiharu Tako [a]
[a] Research Laboratory of Precision Machinery and Electronics, Tokyo Institute of Technology, Nagatsuta-cho, Midori-ku, Yokohama, 227
Version of record first published: 28 Mar 2007.

To cite this article: Tadashi Akahane & Toshiharu Tako (1977): Molecular Alignment of Bubble Domains in Large Pitch Cholesteric Liquid Crystals, Molecular Crystals and Liquid Crystals, 38:1, 251-263

To link to this article: http://dx.doi.org/10.1080/15421407708084391

Mol. Cryst. Liq. Cryst., 1977, Vol. 38, pp. 251–263

Printed in Holland

Molecular Alignment of Bubble Domains in Large Pitch Cholesteric Liquid Crystals

TADASHI AKAHANE and TOSHIHARU TAKO

Research Laboratory of Precision Machinery and Electronics, Tokyo Institute of Technology, Nagatsuta-cho, Midori-ku, Yokohama 227

(*Received August 31, 1976*)

Based on the naive model, the molecular alignment of the bubble domain in large pitch cholesterics is calculated numerically by using the continuum theory of liquid crystals. It is shown that the bubble domain is surely stable under certain conditions but when the cell thickness is thinner than the critical thickness homeotropic alignment is more favourable. The effects of the electric field on the bubble diameter are also investigated. Obtained results agree well qualitatively with the experimental results.

1 INTRODUCTION

A cholesteric liquid crystal exhibits interesting domain textures because of its spiral structure when it is inserted between parallel plates or in a small-angle wedge. For homogeneous molecular alignment (tangential boundary condition), the Grandjean texture is well known[1–3] and this phenomenon is used to determine the pitch of a cholesteric liquid crystal.

For homeotropic molecular alignment (perpendicular boundary condition), a long pitch cholesteric shows complicated domain textures so called finger-print textures.[4] Cladis and Kleman[5] explained these textures in terms of various types of disclinations in cholesterics.[6]

Recently, a new domain pattern which has been called "bubble domain" was observed in large pitch cholesterics.[7–10] The bubble domains appear closely packed in a homeotropically aligned cell when the applied voltage is removed after the electrohydrodynamic turbulence is once induced. In addition to this, isolated bubble domains are often observed with striped domains even before the voltage is applied.

It has been known that the bubble domain exists only when the ratio between the cell thickness d and the pitch P_{00}, d/P_{00}, is within a certain region. But its structure (molecular alignment) has not been studied in detail either theoretically or experimentally.

In the previous paper,[11] we presented the preliminary investigation of the structure of an isolated bubble domain by using the static continuum theory of liquid crystals. It was understood why bubble domains do not appear when the cell thickness becomes thin. In this paper, that investigation will be developed to include the contributions from the core energy of disclinations semi-quantitatively. The dependence of the bubble diameter on the applied voltage will be also examined.

2 MOLECULAR ALIGNMENT OF A BUBBLE DOMAIN

2.1 Naive model

Up to the present, the molecular alignment of a bubble domain has not been made clear. Two models were proposed. Kawachi *et al.*[9] suggested that the bubble domain is a ring of a single striped domain as shown in Figure 1. On the other hand, Bhide *et al.*[10] proposed such a model that there is a bubble domain boundary of an oblate spheroid shape, in which the structure is cholesteric with a helical axis perpendicular to the cell boundary and outside of which the structure is homeotropically aligned nematic.

The latter model seems to be dubious as for the simple form as it is, because there must be a two dimensional disclination at the boundary and it is instable from the consideration of free energy.[12] The former model seems to be more reasonable because the loope domains and even the isolated bubble domains can be seen with the striped domains. The following calculation is based on this model.

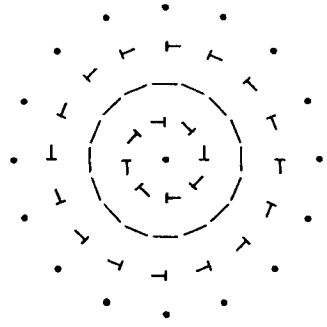

FIGURE 1 Model of the molecular alignment of the bubble domain.

2.2 Molecular alignment

For the model shown in Figure 1, the director **n** which represents the mean direction of the longer axes of molecules can be written as

$$\begin{cases} n_r = 0 \\ n_\theta = -\sin\alpha(r, z) \\ n_z = \cos\alpha(r, z) \end{cases} \tag{1}$$

in the cylindrical coordinate system, where z-axis is perpendicular to the boundary plane and α is the angle between z-axis and **n**.

Let us find α as a function of r and z which minimizes the free energy of the bubble domain. The elastic free energy density f of the cholesteric liquid crystal with pitch P_{00} is given by[13]

$$f = \tfrac{1}{2}\{K_{11}(\operatorname{div}\mathbf{n})^2 + K_{22}(\mathbf{n}\cdot\operatorname{curl}\mathbf{n} + q_{00})^2 + K_{33}(\mathbf{n}\times\operatorname{curl}\mathbf{n})^2\} \tag{2}$$

where K_{11}, K_{22} and K_{33} are the elastic constants for three basic types of deformation, splay, twist and bend respectively. In Eq. (2), $q_{00} = 2\pi/P_{00}$. Hereafter, one constant approximation ($K_{11} = K_{22} = K_{33} = K$) is used for the sake of simplicity. Then,

$$f = \frac{K}{2}\{(\operatorname{div}\mathbf{n})^2 + (\mathbf{n}\cdot\operatorname{curl}\mathbf{n} + q_{00})^2 + (\mathbf{n}\times\operatorname{curl}\mathbf{n})^2\}. \tag{2'}$$

Substituting Eq. (1) into Eq. (2'), we obtain

$$f = \frac{K}{2}\left\{\left(\frac{\partial\alpha}{\partial z}\right)^2 + \left(q_{00} - \frac{\partial\alpha}{\partial r} - \frac{1}{r}\sin\alpha\cos\alpha\right)^2 + \frac{\sin^4\alpha}{r^2}\right\}. \tag{3}$$

If the diameter of the bubble domain is P_0 and the cell thickness is d, the elastic free energy F of the bubble domain is given by

$$F = \int_{-d/2}^{d/2} dz \int_0^{P_0/2} dr \int_0^{2\pi} d\theta r f. \tag{4}$$

According to the variational principle, $\alpha(r, z)$ must satisfy the following equation,

$$\frac{\partial^2\alpha}{\partial r^2} + \frac{1}{r}\frac{\partial\alpha}{\partial r} + \frac{\partial^2\alpha}{\partial z^2} - \frac{q_{00}}{r}(1 - \cos 2\alpha) - \frac{1}{2r^2}\sin 2\alpha = 0. \tag{5}$$

The boundary conditions are

$$\begin{cases} \alpha(0, z) = 0 \\ \alpha\left(\frac{P_0}{2}, z\right) = \pi \\ \alpha\left(r, \pm\frac{d}{2}\right) = \pi Y\left(r - \frac{P_0}{4}\right), \end{cases} \tag{6}$$

where $Y(r) = 0$ for $r < 0$ and $Y(r) = 1$ for $r > 0$. In Eq. (6), it is assumed that the disclinations exist at $r = P_0/4$ on the boundary planes. This is the analogy with the case of the striped domain.[5]

Equation (5) is a nonlinear partial differential equation and it is difficult to solve it analytically. So it is solved numerically by means of the finite-difference method.[14] Before doing so, we change variables as

$$\begin{cases} r = \frac{P_0}{2} r_n \\ z = \frac{d}{2} z_n \\ \alpha = \pi\alpha_n \end{cases} \tag{7}$$

and rewrite Eq. (5) by the normalized variables r_n, z_n and α_n as

$$\frac{\partial^2\alpha_n}{\partial r_n^2} + \frac{1}{r_n}\frac{\partial\alpha_n}{\partial r_n} + s^2\frac{\partial^2\alpha_n}{\partial z_n^2} - \frac{st}{r_n}(1 - \cos 2\pi\alpha_n) - \frac{1}{2\pi r_n^2}\sin 2\pi\alpha_n = 0 \tag{8}$$

where

$$\begin{cases} s = P_0/d, \\ t = d/P_{00}. \end{cases} \tag{9}$$

The boundary conditions (6) reduce to

$$\begin{cases} \alpha_n(0, z_n) = 0, \\ \alpha_n(1, z_n) = 1, \\ \alpha_n(r_n, \pm 1) = Y(r_n - \frac{1}{2}). \end{cases} \tag{10}$$

From the consideration of the symmetry of the problem (from Eqs. 8 and 10), α_n is an even function of z_n. Then, it is sufficient to solve Eq. (8) in the region $0 \leqq r_n \leqq 1$ and $0 \leqq z_n \leqq 1$. The way to solve Eq. (8) by means of the finite-difference method is given in Appendix.

Calculated results are shown in Figure 2. For $z_n = 0$ (in the central region of the cell), the twist angle α increases almost linearly as r_n increases. For

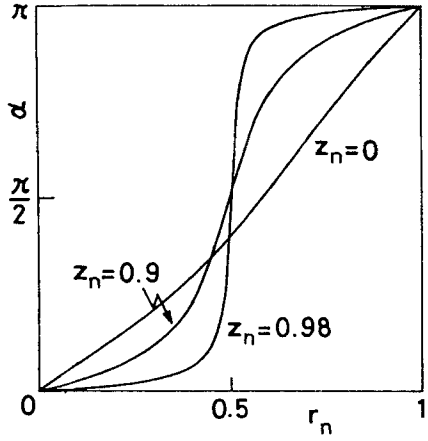

FIGURE 2 α as a function of r_n ($= 2r/P_0$) for different values of z_n ($= 2z/d$).

$z_n = 0.98$ (near the boundary plane), however, α changes abruptly at $r_n \sim 0.5$ (at the disclination).

2.3 Free energy

In Section 2.2, the molecular alignment (twist angle α) has been obtained as a function of position with s ($= P_0/d$) and t ($= d/P_{00}$) as parameters. As the values of P_{00} (pitch of the cholesteric) and d (cell thickness) are known beforehand, the parameter t can be given arbitrary. Then, the problem is to decide the value of P_0 (diameter of the bubble domain) when t is given. To do this, we must obtain the free energy F with s as a parameter for fixed t by substituting the solution obtained in Section 2.2 into Eqs. (3) and (4), and find the value of s which minimize F. From Eqs. (3) and (4),

$$F = \pi^3 Kd \int_0^1 dz_n \int_0^1 dr_n \left\{ s^2 r_n \left(\frac{\partial \alpha_n}{\partial z_n} \right)^2 + r_n \left(st - \frac{\partial \alpha_n}{\partial r_n} - \frac{\sin \pi\alpha_n \cos \pi\alpha_n}{\pi r_n} \right)^2 + \frac{\sin^4 \pi\alpha_n}{\pi^2 r_n} \right\}. \quad (11)$$

From Eq. (11), the free energy for homoetropic molecular alignment ($\alpha_n \equiv 0$), F_h, is given by

$$F_h = \frac{\pi^3 Kds^2 t^2}{2}. \quad (12)$$

Then, the free energy of the bubble domain normalized by F_h can be written as

$$\bar{F} \equiv \frac{F}{F_h} = \frac{2}{s^2 t^2} \int_0^1 dz \int_0^1 dr \left\{ s^2 r \left(\frac{\partial \alpha}{\partial z} \right)^2 + r \left(st - \frac{\partial \alpha}{\partial r} - \frac{\sin \pi\alpha \cos \pi\alpha}{\pi r} \right)^2 + \frac{\sin^4 \pi\alpha}{\pi^2 r} \right\} \quad (13)$$

To evaluate Eq. (13), we approximate differential quotients by differences and use summation in place of integral.

Now, let us consider the extreme neighbourhood of the disclination ($z_n = 1, r_n = \frac{1}{2}$). There the molecular alignment changes abruptly in a few molecular lengths. In such a case, it is not adequate to apply the continuum theory. Therefore, the contribution from this region must be excluded from the integration region of Eq. (13). The free energy in this region must be considered to be the core energy of the disclination.

The core energy, however, is hard to calculate quantitatively.[15] Therefore, we evaluate it only semi-quantitatively. If the intermolecular distance is a and the interaction energy between molecules is U, the core energy of disclination per unit length is considered to be of the order of U/a. On the other hand, the elastic constant K is also of the order of U/a.

On the basis of this discussion, the core energy of the disclinations in the bubble domain is given by

$$F_{\text{dis}} = 2 \times 2\pi \frac{P_0}{4} \times K = \pi K P_0. \quad (14)$$

Normalized by F_h, Eq. (14) reduces to

$$\bar{F}_{\text{dis}} = F_{\text{dis}}/F_h = \frac{2}{\pi^2 s t^2}. \quad (15)$$

Finally, the total free energy of the bubble domain $\bar{F}_{\text{tot}}$ is written as

$$\bar{F}_{\text{tot}} = \bar{F} + \bar{F}_{\text{dis}}. \quad (16)$$

In Eq. (16), $\bar{F}$ is calculated from Eq. (13) by excluding the extreme neighbourhood of the disclination from the integration region. In the case of $t\ (= d/P_{00}) = 1$, $\bar{F}_{\text{tot}}$, $\bar{F}$ and $\bar{F}_{\text{dis}}$ are shown as functions of $s\ (= P_0/d)$ in Figure 3. F_{tot} takes a minimum value at $s = 1.75$. In Figure 4, $\bar{F}_{\text{tot}}$ is shown as a function of s for $t = 0.5$, 1 and 2. As is seen from Figure 4, for a given t, the value of s which minimizes the free energy can be determined uniquely. This value of s and the minimized free energy are shown as functions of t in Figure 5.

It is seen from Figure 5 that $F_{\text{tot}}/F_h > 1$ when $d/P_{00} \lesssim 0.5$. This result means that the homeotropic molecular alignment is more stable than the

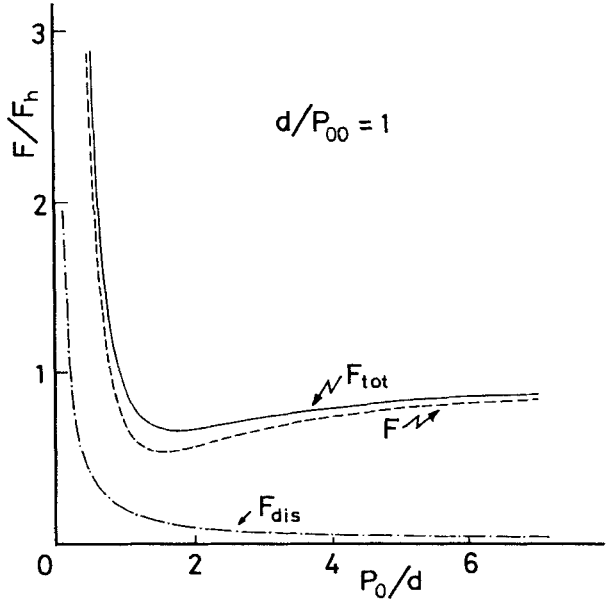

FIGURE 3 $\bar{F}_{tot}$, $\bar{F}$ and $\bar{F}_{dis}$ as function of P_0/d for $d/P_{00} = 1$.

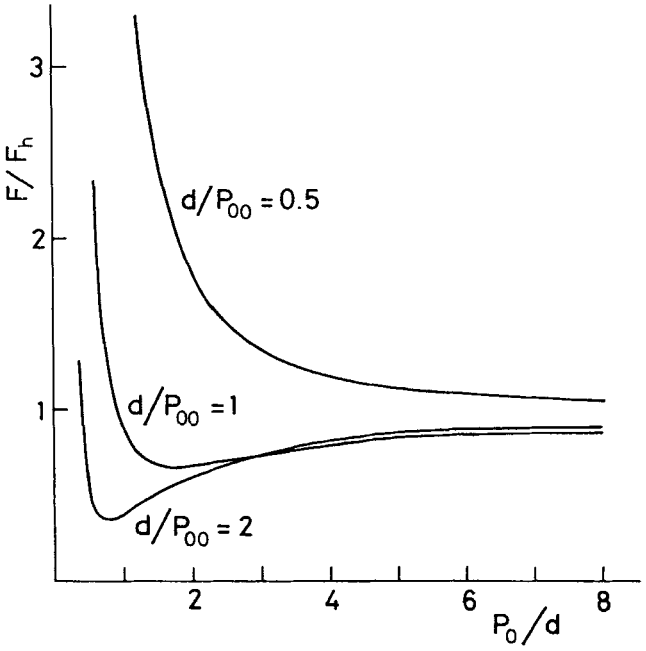

FIGURE 4 F_{tot}/F_h as a function of P_0/d for different values of d/P_{00}.

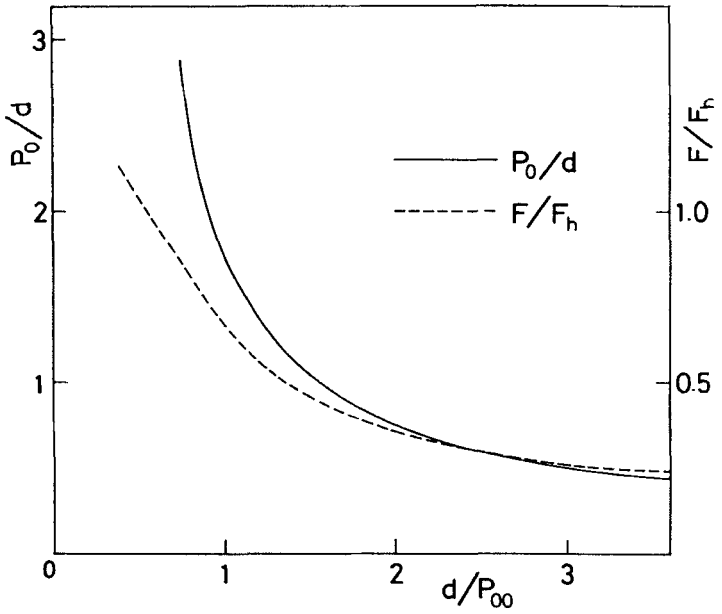

FIGURE 5 P_0/d and F_{tot}/F_h as functions of d/P_{00}.

alignment which forms the bubble domain when $d/P_{00} \lesssim 0.5$. The P_0/d decreases monotonically as d/P_{00} increases. The discussions about these results will be given in Section 3.

2.4 Effects of the electric field on the bubble diameter

It has been known experimentally that the bubble diameter increases for the case of cholesterics with negative dielectric anisotropy (n-type liquid crystals) when voltages are applied on the cell. In this sub-section, it is investigated whether this phenomenon can be explained by the model used here or not.

When the electric field **E** is present, the dielectric free energy density of the liquid crystal is given by

$$f_{\text{diel}} = -\tfrac{1}{2}\varepsilon_a(E \cdot n)^2 = -\tfrac{1}{2}\varepsilon_a E^2 \cos^2 \alpha \tag{17}$$

where $\varepsilon_a = \varepsilon_p - \varepsilon_n$ (ε_p and ε_n are the dielectric constants along and perpendicular to the director **n** respectively). In Eq. (17), the term which is independent on **n** is neglected.

From Eqs. (2′) and (17), the free energy density of a cholesteric when **E** is present is given by

$$f = \frac{K}{2}\{(\operatorname{div}\mathbf{n})^2 + (\mathbf{n}\cdot\operatorname{curl}\mathbf{n} + q_{00})^2 + (\mathbf{n}\times\operatorname{curl}\mathbf{n})^2\} + \frac{\varepsilon_a}{2}E^2\cos^2\alpha. \quad (18)$$

ε_a is negative for n-type liquid crystals. The equation of $\alpha(r, z)$ can be derived in the same way as in Section 2.2 and is given by

$$\frac{\partial^2\alpha}{\partial r^2} + \frac{1}{r}\frac{\partial\alpha}{\partial r} + \frac{\partial^2\alpha}{\partial z^2} - \frac{q_{00}}{r}(1-\cos 2\alpha) - \frac{1}{2r^2}\sin 2\alpha + \frac{|\varepsilon_a|E^2}{2K}\sin 2\alpha = 0. \quad (19)$$

Strictly speaking, **E** is not constant in the dielectrically anisotropic medium like liquid crystals. We assumed, however, that **E** is constant and the applied voltage is given by $V = Ed$ for the sake of simplicity. If we put

$$\pi\sqrt{\frac{K}{|\varepsilon_a|}} = V_0 \qquad \text{and} \qquad \varepsilon = \frac{V}{V_0} \quad (20)$$

Eq. (19) reduce, in terms of normalized variables, to

$$\frac{\partial^2\alpha_n}{\partial r_n^2} + \frac{1}{r_n}\frac{\partial\alpha_n}{\partial r_n} + s^2\frac{\partial^2\alpha_n}{\partial z_n^2} - \frac{st}{r_n}(1-\cos 2\pi\alpha_n) - \frac{\sin 2\pi\alpha_n}{2\pi r_n^2} + \frac{\pi\varepsilon^2 s^2}{8}\sin 2\pi\alpha_n = 0. \quad (21)$$

The free energy of the bubble is given by

$$\bar{F} = \frac{F}{F_n} = \frac{2}{s^2t^2}\int_0^1 dz\int_0^1 dr\left\{s^2 r\left(\frac{\partial\alpha}{\partial z}\right)^2 + r\left(st - \frac{\partial\alpha}{\partial r} - \frac{\sin\pi\alpha\cos\pi\alpha}{\pi r}\right)^2 + \frac{\sin^4\pi\alpha}{\pi^2 r} + \frac{\varepsilon^2 s^2 r}{4}\cos^2\pi\alpha\right\}. \quad (22)$$

We can decide the value of s which minimizes $\bar{F}_{\text{tot}}$ as a function of ε in the same way as in Sections 2.2 and 2.3. The results are shown in Figure 6. The bubble diameter (P_0/d) increases abruptly when $\varepsilon\,(=V/V_0)$ exceeds a certain value. This value of ε differs accordingly to the value of $t\,(=d/P_{00})$.

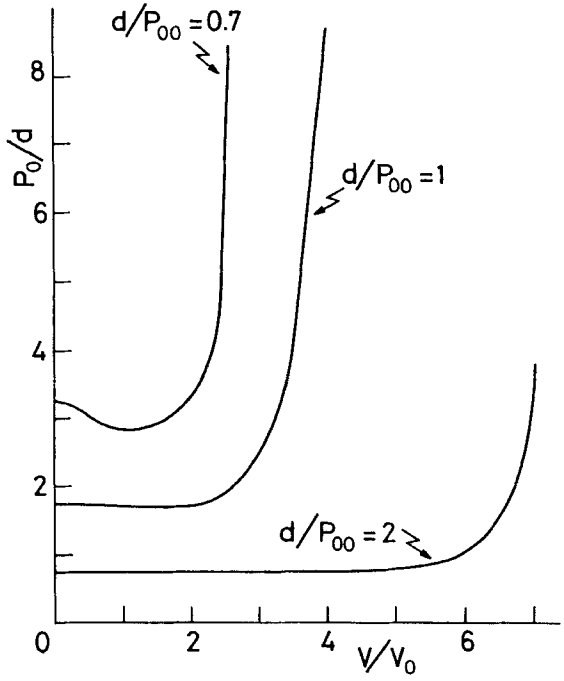

FIGURE 6 P_0/d as a function of V/V_0 for different values of d/P_{00}.

3 DISCUSSIONS AND CONCLUSIONS

In Section 2.2, the molecular alignment of the bubble domain was calculated on the basis of the model shown in Figure 1. Experimentally, the actual structure of the bubble domain has not been made clear up to the present. If the distribution of the refractive index in the bubble domain is obtained by some method, it will give useful information about this point.

In Section 2.3, it was shown that the homeotropic alignment is more stable than the alignment which forms the bubble domain when $d/P_{00} \lesssim 0.5$. This result agrees well with the experimental results made by Bhide *et al.*[10] not only qualitatively but also quantitatively. This quantitative agreement seems to be rather accidental and need not be overestimated because the investigation developed in this paper is based on one constant approximation and the semi-quantitative treatment of the core energy of the disclinations. The more important fact is that the interactions between bubble domains was not taken into account in this investigation. Experimentally, bubble domains were observed to be closely packed. Therefore, these interactions must be taken into account for the completely quantitative comparisons with the

experimental results. The most important conclusion of this work is that the bubble domain is surely stable under certain conditions but when the cell thickness is thinner than the critical thickness homeotropic alignment is more favourable.

In Section 2.4, the effects of the electric field on the bubble diameter were investigated. The qualitative agreement with the experimental results was good. For some values of d/P_{00} ($d/P_{00} = 0.7$ in Figure 6), however, the bubble diameter once decreases and then increases abruptly as the applied voltage increases. Experimentally, this phenomenon has not been reported. It is not clear that this result is due to the simplification of the theory mentioned above or not.

Appendix

Here we describe the finite-difference method[14] to solve Eq. (8). We start by dividing the region $0 \leqq r_n \leqq 1$ and $0 \leqq z_n \leqq 1$ into $N \times N$ cells as shown in Figure 7, where N is an even integer. Then, differential quotients are approximated by differences as

$$\left(\frac{\partial^2\alpha}{\partial r^2}\right)_{mh,\,nh} = h^{-2}\{\alpha((m+1)h, nh) - 2\alpha(mh, nh) + \alpha((m-1)h, nh)\}$$

$$\left(\frac{\partial^2\alpha}{\partial z^2}\right)_{mh,\,nh} = h^{-2}\{\alpha(mh, (n+1)h) - 2\alpha(mh, nh) + \alpha(mh, (n-1)h)\} \quad \text{(A.1)}$$

$$\left(\frac{\partial\alpha}{\partial r}\right)_{mh,\,nh} = (2h)^{-1}\{\alpha((m+1)h, nh) - \alpha((m-1)h, nh)\}$$

where $h = 1/N$ and m, n are integers from 1 to $N - 1$. Here, the suffix n which denotes the normalized variables is omitted.

Substituting Eq. (A.1) into Eq. (8), we obtain

$$\alpha_{m,n} = \frac{1}{2(1+s^2)}\left\{\left(1 + \frac{1}{2m}\right)\alpha_{m+1,n} + \left(1 - \frac{1}{2m}\right)\alpha_{m-1,n} + \alpha_{m,n-1}\right)$$
$$- \frac{sth}{m}(1 - \cos 2\pi\alpha_{m,n}) - \frac{1}{2\pi m^2}\sin 2\pi\alpha_{m,n}\Bigg\} \quad \text{(A.2)}$$

where $\alpha_{m,n} = \alpha(mh, nh)$. There are $(N+1)^2$ lattice points in Figure 7. The values of $\alpha_{m,n}$ at these lattice points must be solved. Among them, $\alpha_{m,n}$ at the lattice points on the boundary are given by the boundary conditions, Eq. (10). So, we are left with $(N-1)^2$ unknown $\alpha_{m,n}$. If the original partial

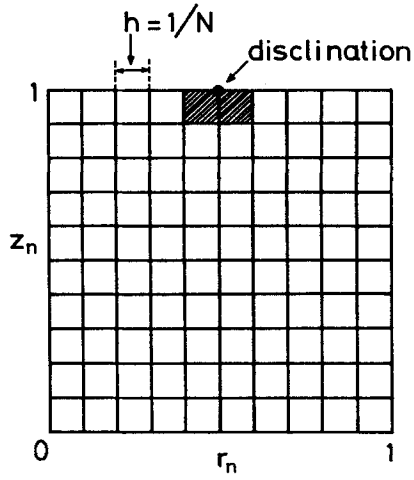

FIGURE 7 Lattice for numerical calculations by means of the finite-difference method.

differential equation is linear, the derived difference equation reduces to linear system with respect to the $(N-1)^2$ unknown $\alpha_{m,n}$. Equation (A.2), however, is not linear. So, we solve it by means of the itterative method. As the 0-th order solutions, we take homogeneous twist, that is,

$$\alpha^{(0)}_{m,n} = hm; \qquad 1 \leqq m, n \leqq N-1. \tag{A.3}$$

The first order solution can be obtained by substituting (A.3) into Eq. (A.2), and so on.

In general, the error when the partial differential equation is replaced by the finite-difference equation is considered to be of the order of $1/N^2$. On the other hand, the error of the iterative method can be made arbitrarily small. The results shown in Figure 2 were obtained by taking $N = 50$.

In obtaining the free energy of the bubble domain, we further divide the two cells near the disclination (denoted by hatch in Figure 7) into $M \times M$ sub-cells respectively and exclude the contributions from the two sub-cells near the disclination. The results shown in Figures 3 to 6 are obtained by taking $N = 20$ and $M = 10$.

References

1. F. Grandjean, *C. R. Acad. Sci.*, **172**, 71 (1921).
2. R. Cano, *Bull. Soc. Franc. Mineral. Crist.*, **91**, 20 (1968).
3. P. Kassubeck and G. Meier, *Mol. Cryst. Liq. Cryst.*, **8**, 305 (1969).
4. I. Rault and P. E. Cladis, *Mol. Cryst. Liq. Cryst.*, **15**, 1 (1971).
5. P. E. Cladis and M. Kleman, *Mol. Cryst. Liq. Cryst.*, **16**, 1 (1972).
6. M. Kleman and J. Friedel, *J. de Physique*, **30C**, 4 (1969).

7. W. E. L. Haas and J. E. Adams, *Appl. Phys. Lett.*, **25**, 263 (1974).
8. W. E. L. Haas and J. E. Adams, *Appl. Phys. Lett.*, **25**, 535 (1974).
9. M. Kawachi, O. Kogure, and Y. Kato, *Japan. J. Appl. Phys.*, **13**, 1457 (1974).
10. V. G. Bhide, S. Chandra, S. C. Jain, and R. K. Medhekar, *J. Appl. Phys.*, **47**, 120 (1976).
11. T. Akahane and T. Tako, *Japan. J. Appl. Phys.*, **15**, 1559 (1976).
12. P. G. de Gennes, *The Physics of Liquid Crystals* (Clarendon Press, Oxford, 1974) p. 127.
13. F. C. Frank, *Disc. Faraday Soc.*, **25**, 19 (1958).
14. G. E. Forsythe and W. R. Wasow, *Finite-Difference Method for Partial Differential Equations* (John Wiley and Sons, Inc., New York, 1960).
15. See Ref. 12, p. 131.